Modeling of the Lyman-α forest and weak lensing detector systematics

Jahmour Givans

Berkeley Cosmology Group Meeting

November 17, 2020

THE OHIO STATE UNIVERSITY

Part I: Lyα forest

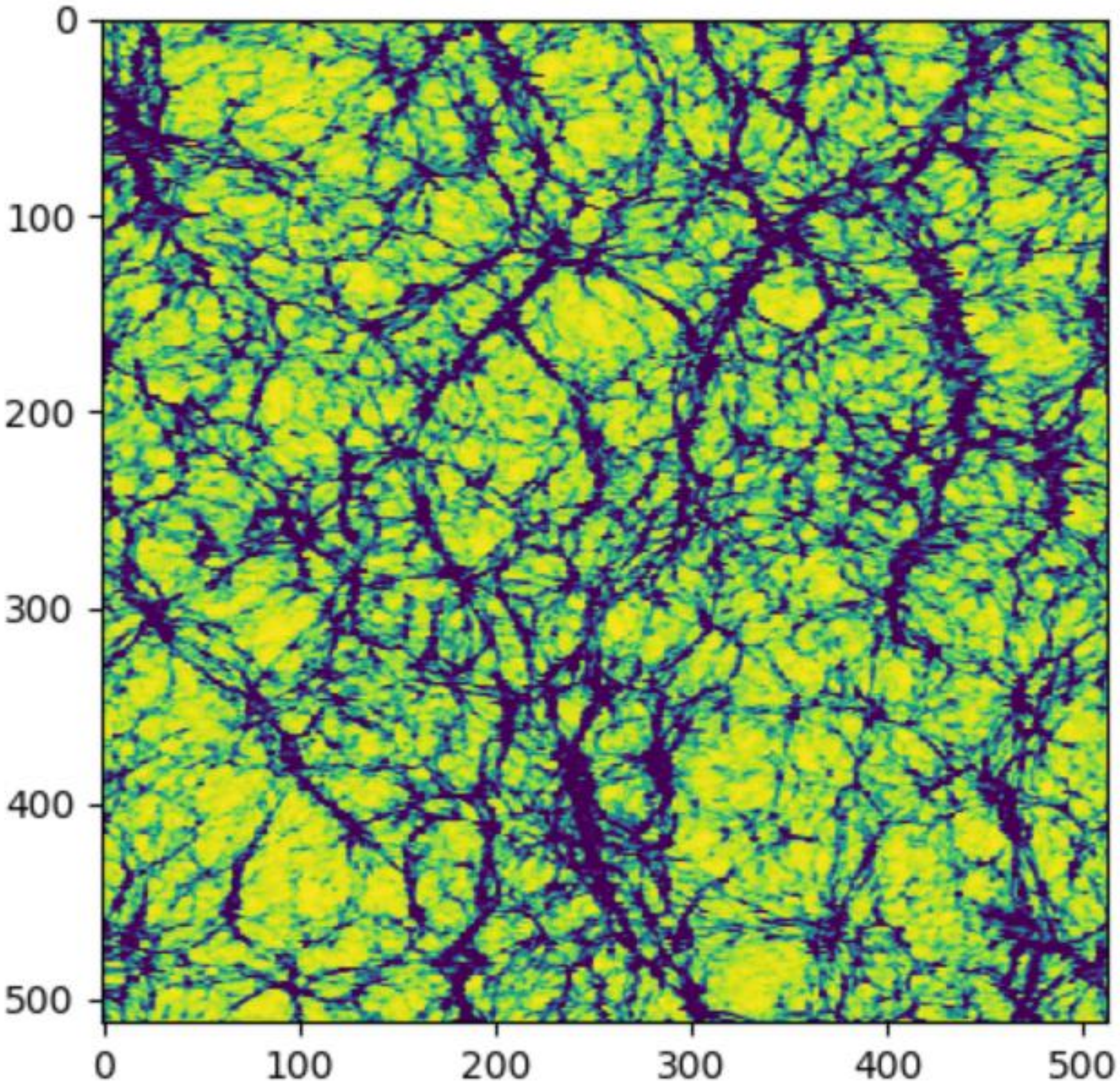

Based on . . .

PHYSICAL REVIEW D **102**, 023515 (2020)

Redshift-space streaming velocity effects on the Lyman-α forest baryon acoustic oscillation scale

Jahmour J. Givans[1,2,*] and Christopher M. Hirata[1,2,3]

[1]*Center for Cosmology and AstroParticle Physics, The Ohio State University, 191 West Woodruff Avenue, Columbus, Ohio 43210, USA*
[2]*Department of Physics, The Ohio State University, 191 West Woodruff Avenue, Columbus, Ohio 43210, USA*
[3]*Department of Astronomy, The Ohio State University, 140 West 18th Avenue, Columbus, Ohio 43210, USA*

(Received 6 March 2020; accepted 8 June 2020; published 8 July 2020)

The baryon acoustic oscillation (BAO) scale acts as a standard ruler for measuring cosmological distances and has therefore emerged as a leading probe of cosmic expansion history. However, any physical effect that alters the length of the ruler can lead to a bias in our determination of distance and expansion rate. One of these physical effects is the streaming velocity, the relative velocity between baryons and dark matter in the early Universe, which couples to the BAO scale due to their common origin in acoustic waves at recombination. In this work, we investigate the impact of streaming velocity on the BAO feature of the Lyman-α forest auto-power spectrum, one of the main tracers being used by the recently commissioned Dark Energy Spectroscopic Instrument (DESI). To do this, we develop a perturbative model for Lyman-α flux fluctuations which is complete to second order for a certain set of fields, and applicable to *any* redshift-space tracer of structure since it is based only on symmetry considerations. We find that there are 8 biasing coefficients through second order. We find streaming velocity-induced shifts in the BAO scale of 0.081%–0.149% (transverse direction) and 0.053%–0.058% (radial direction), depending on the model for the biasing coefficients used. These are smaller than, but not negligible compared to, the DESI Lyman-α BAO error budget, which is 0.46% on the overall scale. The sensitivity of these results to our choice of bias parameters underscores the need for future work to measure the higher-order biasing coefficients from simulations, especially for future experiments beyond DESI.

DOI: 10.1103/PhysRevD.102.023515

Breaking down the paper title

Over the next several slides, we'll address

- Redshift space
- Baryon acoustic oscillations (BAOs)
- Streaming velocity
- Lyman-α forest

Redshift space

- In real space, objects (like galaxies) are where they appear to be.
- In redshift space, an object's position is distorted along our LOS
  - Caused by peculiar velocities
  - Convention is that line-of-sight lies along the z axis

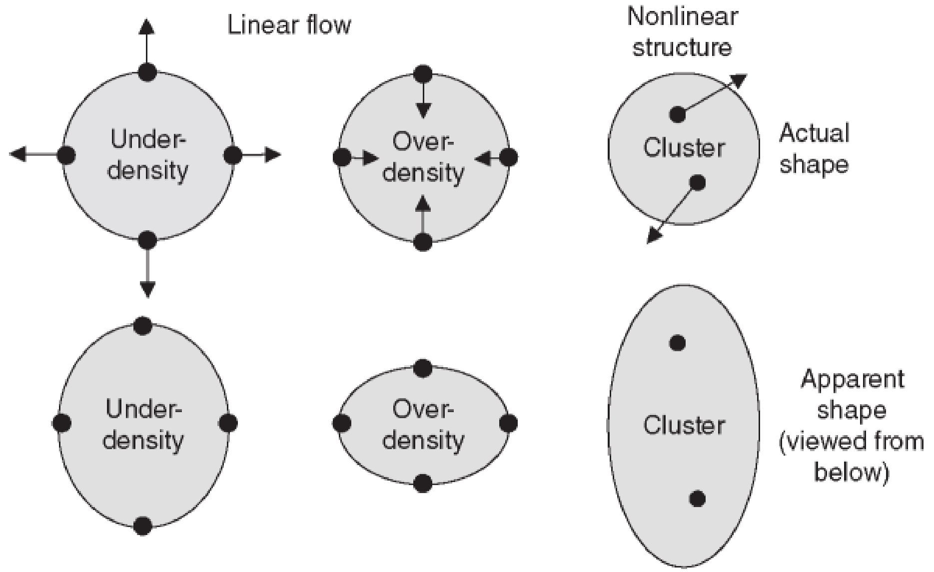

Image credit: Will Percival

BAOs

- Primordial universe is a plasma of photons and baryons
  - Dark matter overdensities are seeded throughout
- Tug-of-war between gravity and fluid pressure
- Generates sound waves called BAOs
  - Can travel a distance $r_d = 147$ comoving Mpc before decoupling
  - Baryons left behind in spherical shell around overdensities
- We get a standard ruler!

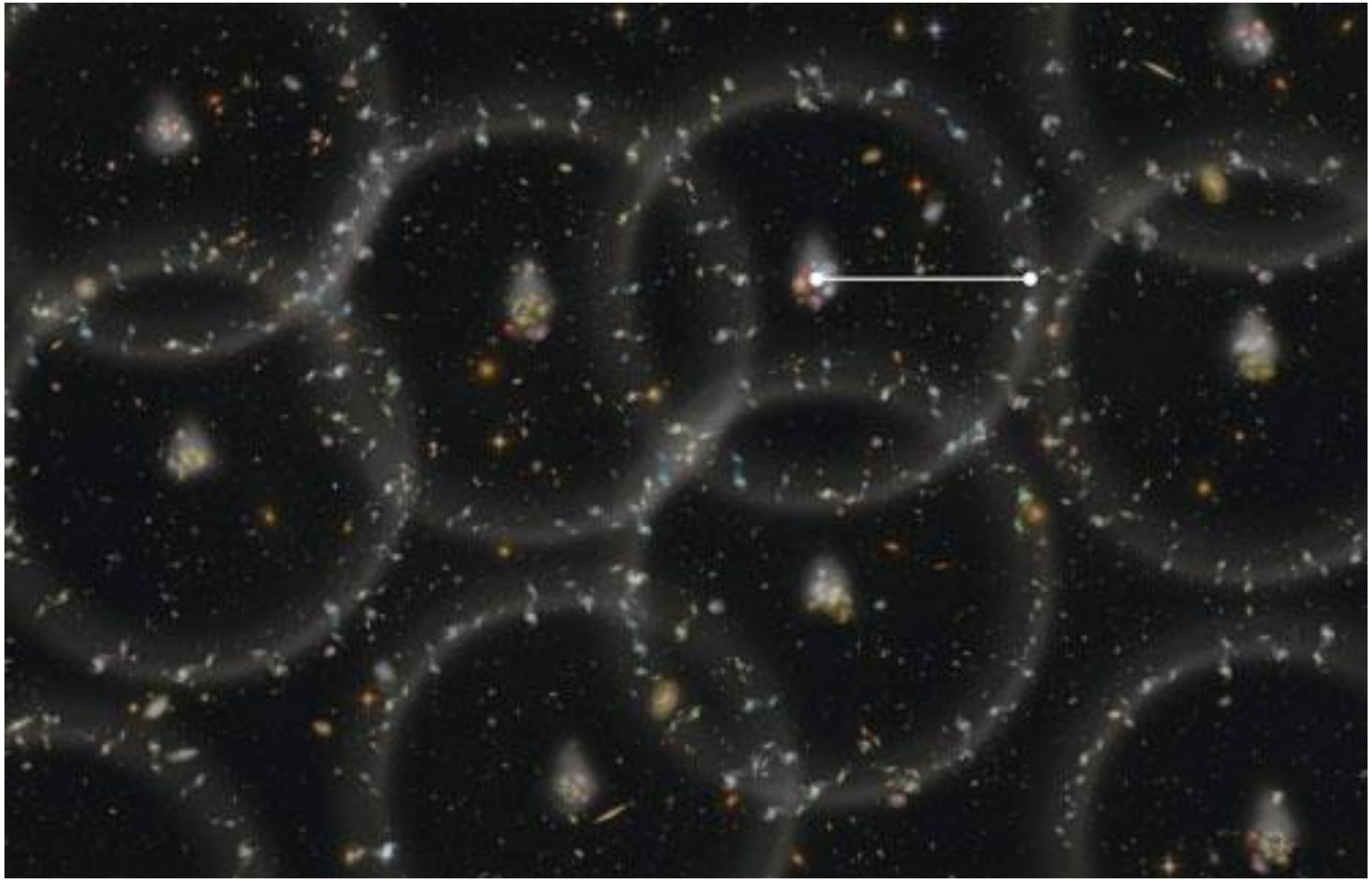

Credit: BOSS Collaboration

Streaming velocity

- Generated by the same physics that produced BAOs
- Baryons and dark matter have a supersonic relative velocity at decoupling
- More important than usual Jeans criteria for structure formation
  - Changes filtering mass of the intergalactic medium
- Will impact the BAO scale by some amount

Lyman-α forest overview

- H I gas clouds spread throughout IGM
- Background quasar shines light, exciting Lyman-α transition
- Absorption in multiple H I clouds along LOS
- Creates a “forest” of absorption features in transmitted flux

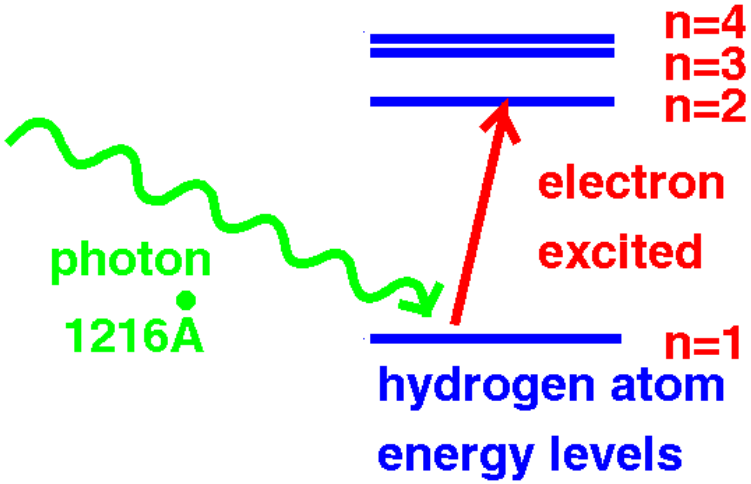

Credit: M. White and L. Hernquist

Visualizing the forest

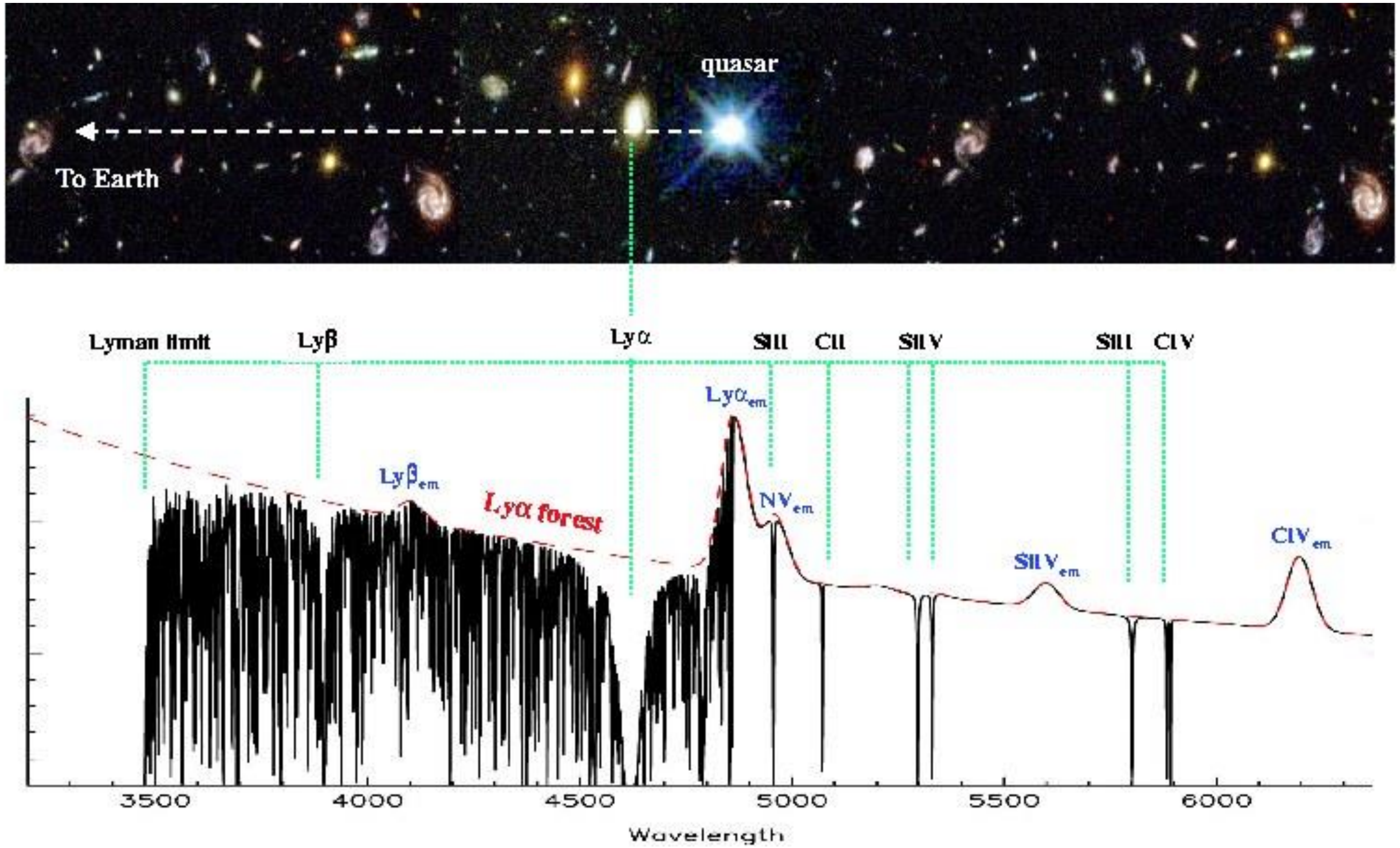

Credit: John Webb

Why the Lyman-α forest?

- Robust tracer of structure at $2 < z < 6$
- Study reionization & thermal history of IGM
- Probe smaller physical scales
- Complement data from other probes

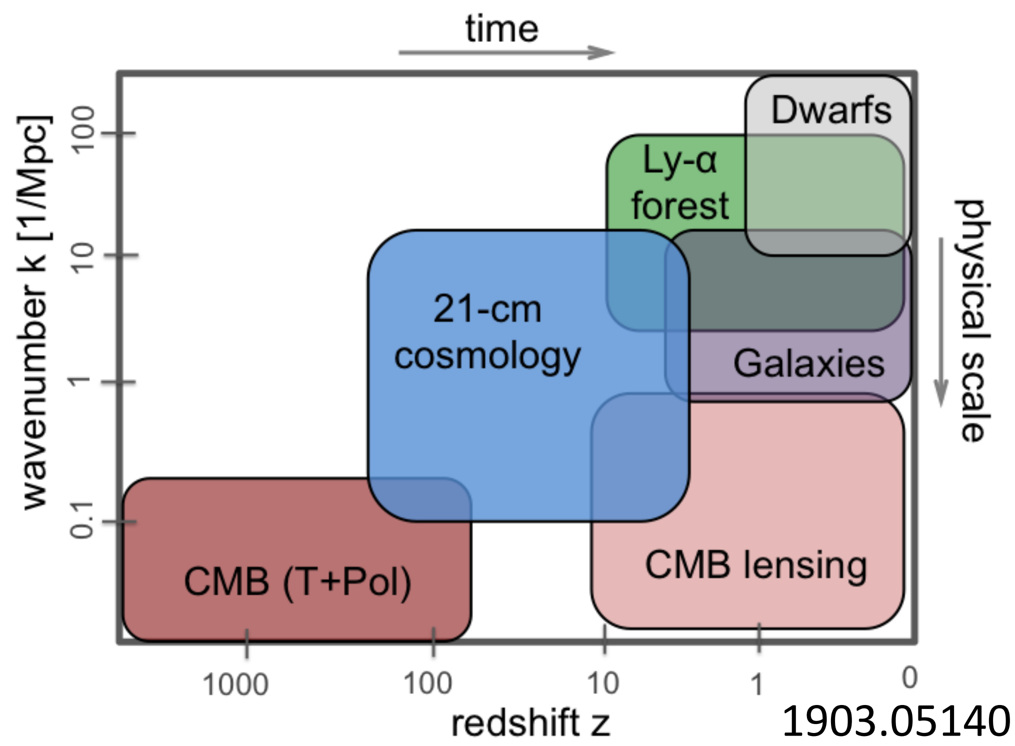

1903.05140

LSS perturbation theory basics

- Assume underlying matter field smooth, collisionless DM
  - Follows Poisson, continuity, and Euler equations
- At large scales, some fields can be treated as perturbations to others

These fields are perturbations	To these local fields
Density contrast	Cosmic density
Peculiar velocity	Particle velocity
Cosmological gravitational potential	Newtonian potential

- Linearize equations to solve for evolution of fields

Biasing theory

- Tracers are related to matter field according to some equation
- Often a messy relationship, but we simplify it into a polynomial
- Set the tracer density contrast equal to fields related to the matter field
- Unknown coefficients are referred to bias coefficients

PT and bias in Lyα forest

- Most (purely) PT models are based on linear theory

$$\delta_F = b_\delta \delta + b_\eta \eta$$

- My work introduced a complete 2nd order model
  - Applicable to any tracer in redshift space
  - Independently derived, but resembles EFT of LSS for galaxies

$$\delta_F(\boldsymbol{s}) = c_0 + c_1\delta + c_2 s_{zz} + c_3\delta^2 + c_4 s^2 + c_5\delta s_{zz} + c_6 t_{zz} + c_7 s_{zz}^2 + c_8\left(s_{xz}^2 + s_{yz}^2\right)$$

- Streaming velocity contributions added

$$b_v(v_s^2 - 1) + b_{1v}\delta(v_s^2 - 1) + b_{sv} s_{ij} v_{s,i} v_{s,j} + b_{vz}\left(v_{s,z}^2 - \frac{1}{3} v_s^2\right)$$

Where did $\delta_F(s)$ come from?

- Get a physical picture of the situation
- Ask what symmetries are present (azimuthal symmetry)
- Consider all relevant fields
- Use group theory!
- Prove our expansion is the most general one possible for fields we consider

Physical picture

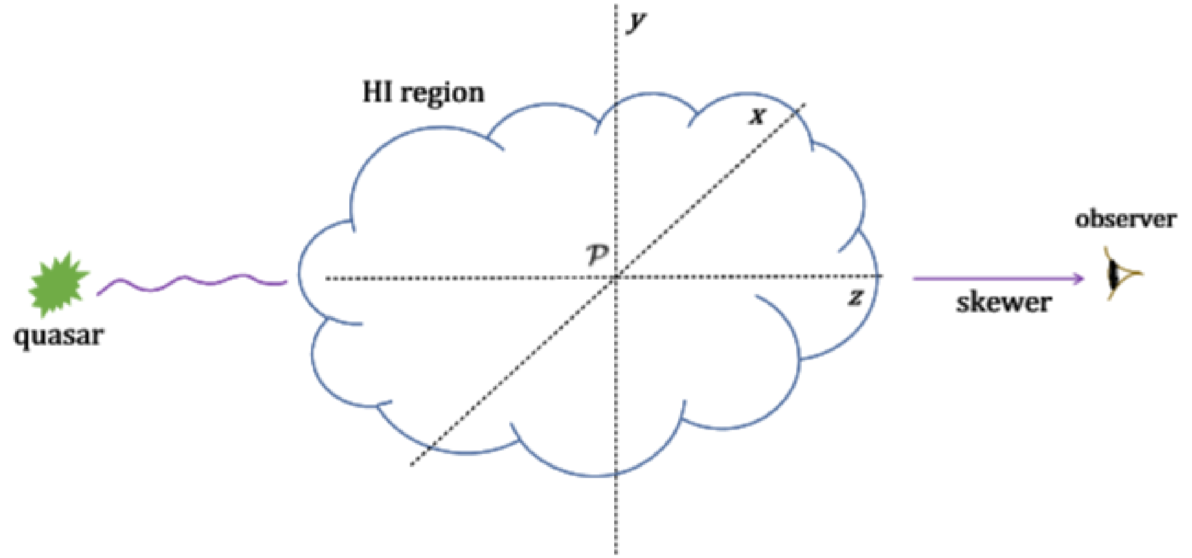

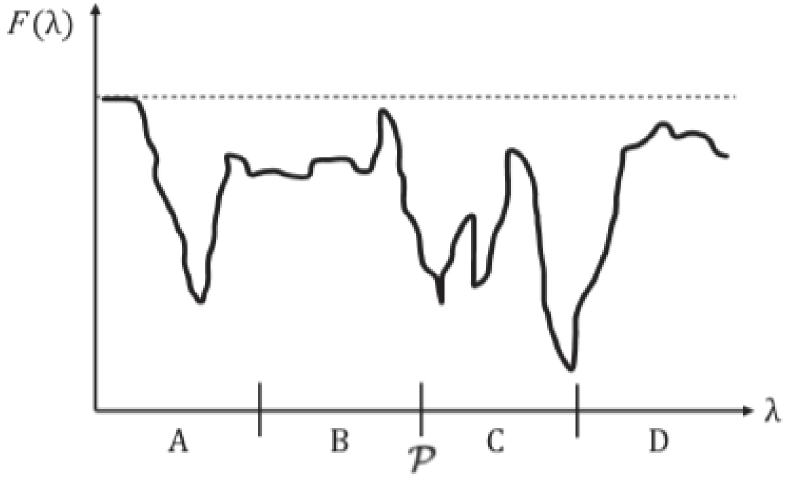

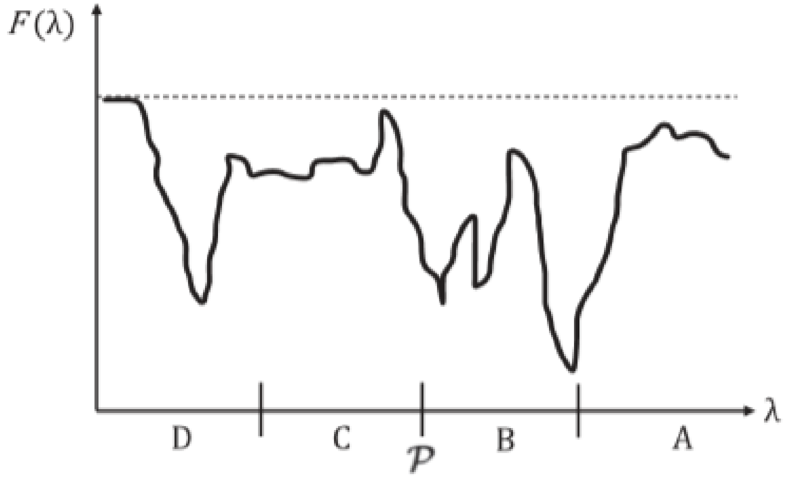

What group is this?

- System obeys group properties of $D_{\infty h}$
  - True if your region is over a very small redshift range
  - Same group that describes symmetry transformation of H_2 and CO_2
- Use a character table to get forms of contributions

$D_{\infty h}$	$\hat{E}$	$2\hat{C}_\infty^\varphi$	$\cdots$	$\infty\hat{\sigma}_v$	$\hat{i}$	$\hat{\sigma}_h$	$2\hat{S}_\infty^\varphi$	$\cdots$	$\infty\hat{C}_2$	linear functions & rotations	quadratic functions
Σ_g^+	$+1$	$+1$	$\cdots$	$+1$	$+1$	$+1$	$+1$	$\cdots$	$+1$	-	x^2+y^2, z^2
Σ_g^-	$+1$	$+1$	$\cdots$	-1	$+1$	$+1$	$+1$	$\cdots$	-1	R_z	-
Π_g	$+2$	$+2\cos\varphi$	$\cdots$	0	$+2$	-2	$-2\cos\varphi$	$\cdots$	0	(R_x, R_y)	(xz, yz)
Δ_g	$+2$	$+2\cos 2\varphi$	$\cdots$	0	$+2$	$+2$	$+2\cos 2\varphi$	$\cdots$	0	-	(x^2-y^2, xy)
Φ_g	$+2$	$+2\cos 3\varphi$	$\cdots$	0	$+2$	-2	$-2\cos 3\varphi$	$\cdots$	0	-	-
$\cdots$	$\cdots$	$\cdots$	$\cdots$	$\cdots$	$\cdots$	$\cdots$	$\cdots$	$\cdots$	$\cdots$	-	-
E_{ng}	$+2$	$+2\cos n\varphi$	$\cdots$	0	$+2$	$(-1)^n 2$	$(-1)^n 2\cos n\varphi$	$\cdots$	0	-	-
$\cdots$	$\cdots$	$\cdots$	$\cdots$	$\cdots$	$\cdots$	$\cdots$	$\cdots$	$\cdots$	$\cdots$	-	-
Σ_u^+	$+1$	$+1$	$\cdots$	$+1$	-1	-1	-1	$\cdots$	-1	z	-
Σ_u^-	$+1$	$+1$	$\cdots$	-1	-1	-1	-1	$\cdots$	$+1$	-	-
Π_u	$+2$	$+2\cos\varphi$	$\cdots$	0	-2	$+2$	$+2\cos\varphi$	$\cdots$	0	(x, y)	-
Δ_u	$+2$	$+2\cos 2\varphi$	$\cdots$	0	-2	-2	$-2\cos 2\varphi$	$\cdots$	0	-	-
Φ_u	$+2$	$+2\cos 3\varphi$	$\cdots$	0	-2	$+2$	$+2\cos 3\varphi$	$\cdots$	0	-	-
$\cdots$	$\cdots$	$\cdots$	$\cdots$	$\cdots$	$\cdots$	$\cdots$	$\cdots$	$\cdots$	$\cdots$	-	-
E_{nu}	$+2$	$+2\cos n\varphi$	$\cdots$	0	-2	$(-1)^{n+1} 2$	$(-1)^{n+1} 2\cos n\varphi$	$\cdots$	0	-	-
$\cdots$	$\cdots$	$\cdots$	$\cdots$	$\cdots$	$\cdots$	$\cdots$	$\cdots$	$\cdots$	$\cdots$	-	-

Getting bias coefficients and BAO scale shift

- A few of them come from simulations
- Others are derived from fluctuating Gunn-Peterson approximation
  - Formula for deriving optical depth in redshift space
  - Optical depth is related to flux, which is related to δ_F
- BAO scale parameter α is set by fitting a model to $P_F(k)$
  - Uses χ^2 minimization to calculate fitting coefficients
  - Compare α when $b_v = 0$ to α when b_v is the simulated value

Visualizing the shift

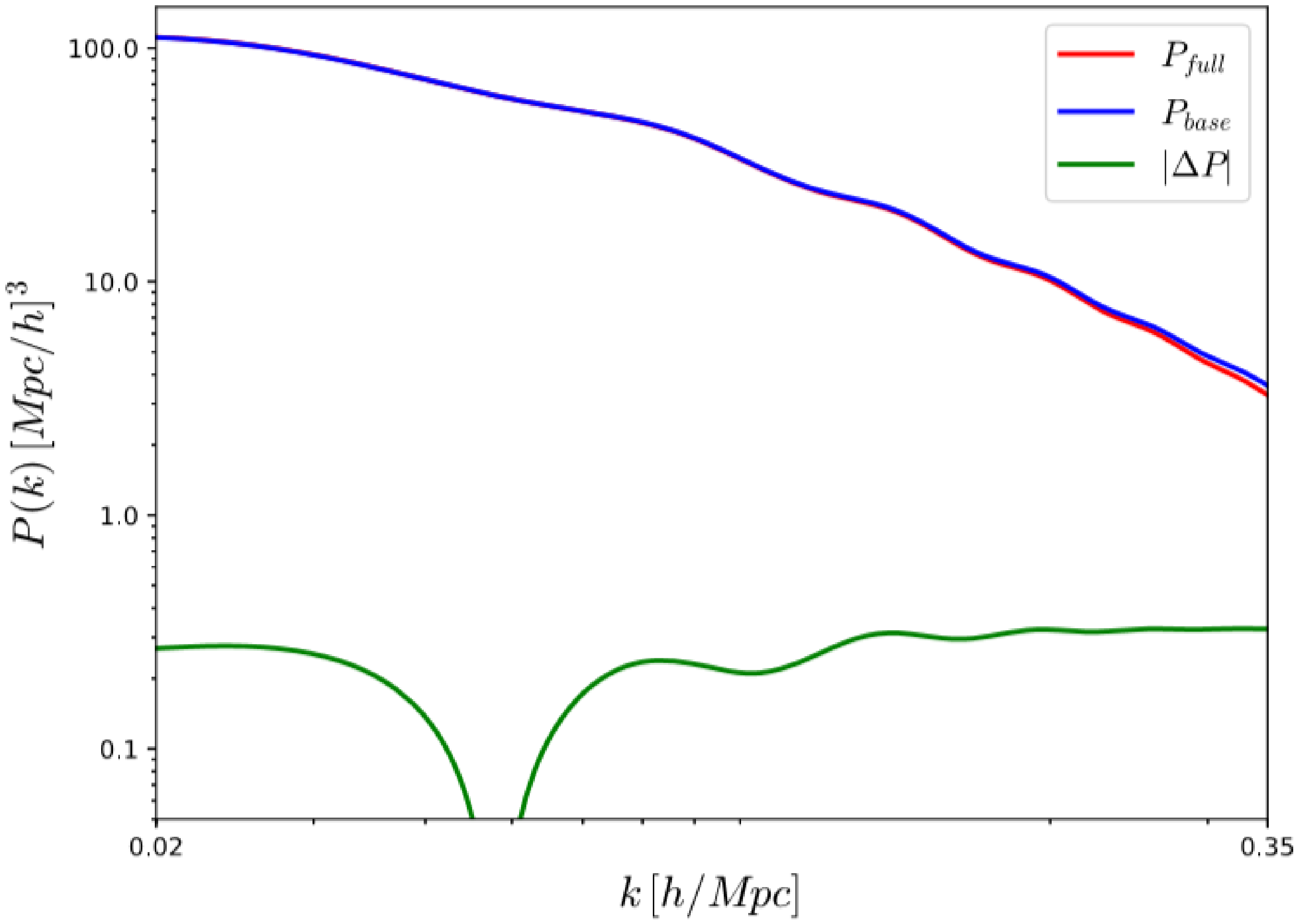

Paper results and takeaways

TABLE III. The BAO peak shift for three different μ values and three different choices of bias coefficients.

$\Delta\alpha$ in %	c_1, c_2, and c_3 from simulations, all others are zero	c_1 and c_2 from simulations, all others are zero	c_1 and c_2 from simulations, all others from FGPA
$\mu = 0$	0.081%	0.088%	0.149%
$\mu = 1/\sqrt{3}$	0.066%	0.070%	0.093%
$\mu = 1$	0.053%	0.054%	0.058%

- Results for peak shift depend strongly on bias parameters
- DESI precision for Lyman-α forest is 0.46%
    - Streaming velocity alone is important but relatively minor
- Go to higher order PT and get bias parameters

Part II: Weak lensing detector systematics

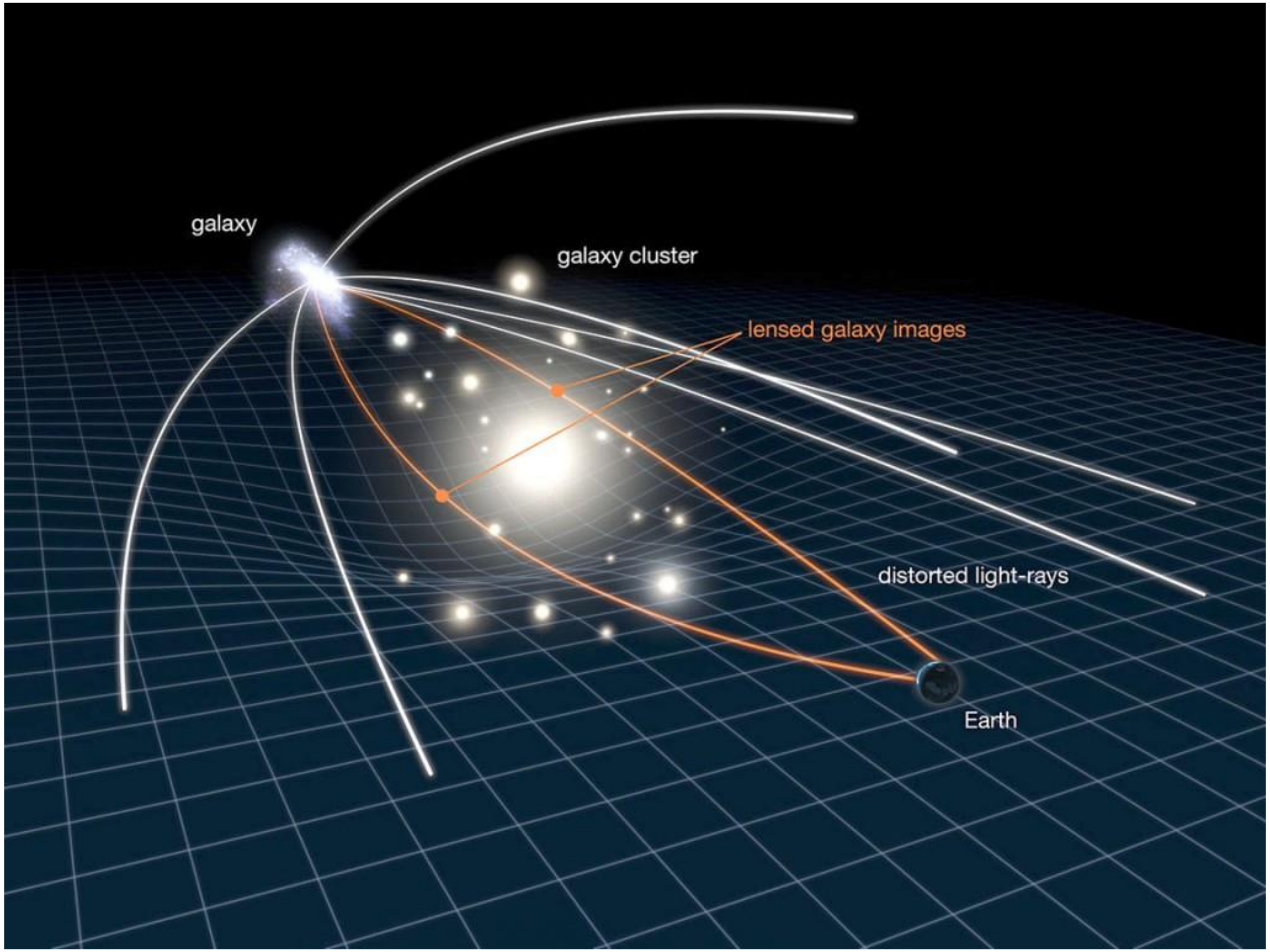

Credit: NASA/ESA

Based on . . .

Publications of the Astronomical Society of the Pacific, 132:074504 (26pp), 2020 July
https://doi.org/10.1088/1538-3873/ab9503

CrossMark

Brighter-fatter Effect in Near-infrared Detectors—III. Fourier-domain Treatment of Flat Field Correlations and Application to WFIRST

Jenna K. C. Freudenburg[1,2], Jahmour J. Givans[2,3], Ami Choi[2,3], Christopher M. Hirata[1,2,3], Chris Bennett[4], Stephanie Cheung[4], Analia Cillis[4], Dave Cottingham[4], Robert J. Hill[4], Jon Mah[4], and Lane Meier[4]

[1] Department of Astronomy, The Ohio State University, 140 West 18th Avenue, Columbus, OH 43210, USA; freudenburg.2@osu.edu
[2] Center for Cosmology and AstroParticle Physics, The Ohio State University, 191 West Woodruff Avenue, Columbus, OH 43210, USA
[3] Department of Physics, The Ohio State University, 191 West Woodruff Avenue, Columbus, OH 43210, USA
[4] NASA Goddard Space Flight Center, Detector Characterization Laboratory, 8800 Greenbelt Rd., Greenbelt, MD 20771, USA

Received 2020 March 24; accepted 2020 May 19; published 2020 June 16

Abstract

Weak gravitational lensing has emerged as a leading probe of the growth of cosmic structure. However, the shear signal is very small and accurate measurement depends critically on our ability to understand how non-ideal instrumental effects affect astronomical images. The Wide-Field Infrared Survey Telescope (WFIRST) will fly a focal plane containing 18 Teledyne H4RG-10 near-infrared detector arrays, which present different instrument calibration challenges from previous weak lensing observations. Previous work [Paper I: Hirata & Choi, PASP, 132, 014501 (2020); and Paper II: Choi & Hirata, PASP, 132, 014502 (2020)] has shown that correlation functions of flat field images, including cross-correlations between different time slices that are enabled by the non-destructive read capability of the infrared detectors, are effective tools for disentangling linear and nonlinear inter-pixel capacitance (IPC) and the brighter-fatter effect (BFE). Here we present a Fourier-domain treatment of the flat field correlations, which allows us to expand the previous formalism to all orders in IPC, BFE, and classical nonlinearity. We show that biases in simulated flat field analyses in Paper I are greatly reduced through the use of this formalism. We then apply this updated formalism to flat field data from three WFIRST flight candidate detectors, and explore the robustness to variations in the analysis. We find that the BFE is present in all three detectors, and that its contribution to the flat field correlations dominates over the nonlinear IPC, in accordance with the results from Paper II on a development detector. The magnitude of the BFE is such that the effective area of a pixel is increased by $(3.54 \pm 0.03) \times 10^{-7}$ for every electron deposited in a neighboring pixel (sensor chip assembly [SCA] 20829, statistical error, not IPC-deconvolved). We compare IPC maps from flat field autocorrelation measurements to those obtained from the single pixel reset method and find a median difference of 0.113% for SCA 20829. After further diagnosis of this difference, we ascribe it largely to an additional source of cross-talk, the vertical trailing pixel effect, and recommend further work to develop a model for this effect. These results represent a significant step toward calibration of the non-ideal effects in WFIRST detectors.

Key words: astronomical instrumentation

Online material: color figures

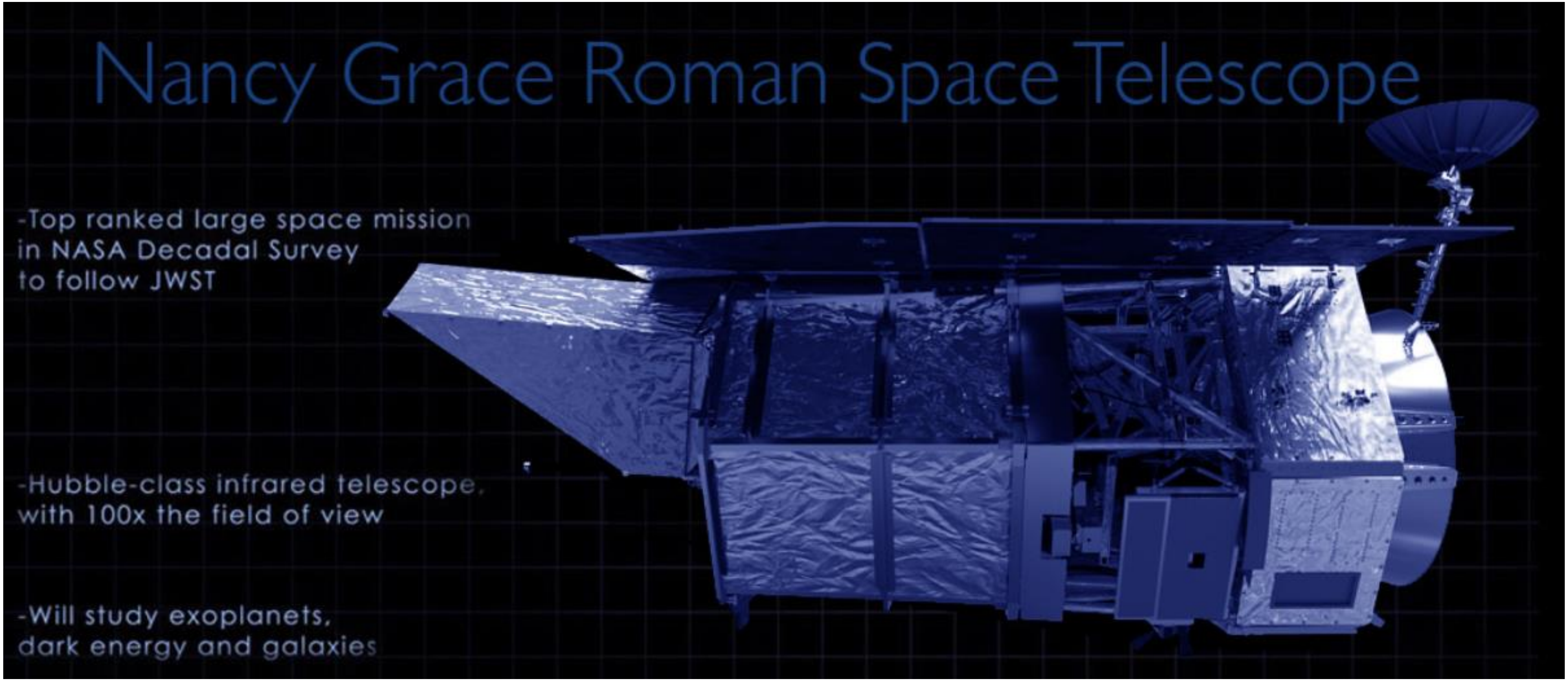

Credit: NASA’s Goddard Space Flight Center

Roman detectors

- 18 CMOS detector arrays
  - Teledyne H4RG-10 readout circuit hybridized to HgCdTe layer
- Non-destructive readout, unlike CCDs
  - Allows sampling of the detector at multiple points in time
- First time these will be applied to LSS weak lensing!

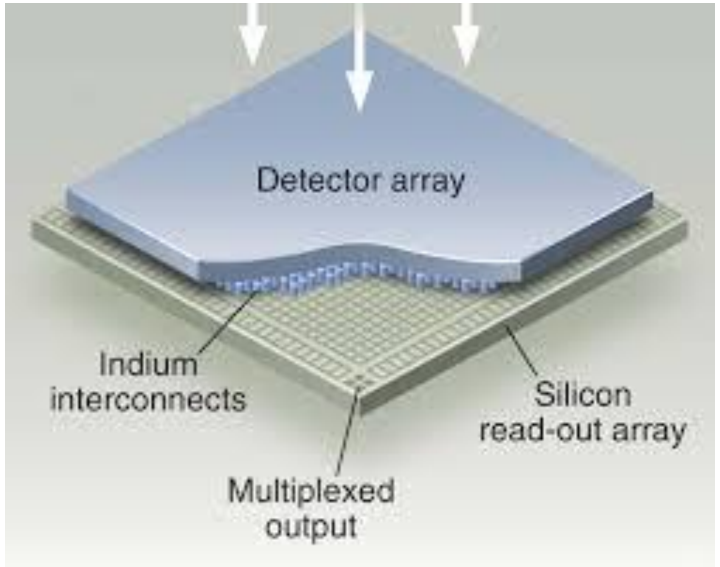

Credit: James Beletic

H4RG-10

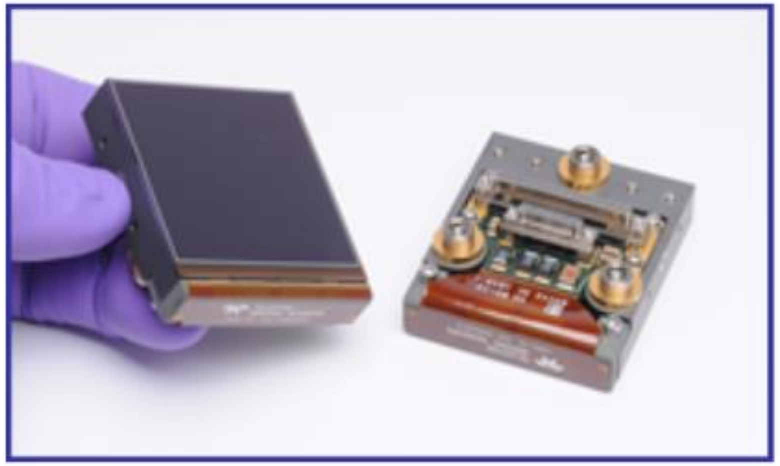

4096×4096, 10 μm pitch

Credit: Auyeung et al 2015

What are the effects?

- Classical nonlinearity (CNL)
  - The nonlinear relationship between accumulated charge and a signal drop
- Interpixel capacitance (IPC)
  - Parasitic capacitance between neighboring pixels
- Brighter-fatter effect (BFE)
  - Change in the effective area of a pixel based on charge in neighbors
  - Follows from Coulomb repulsion
- They all combine as interpixel nonlinearity (IPNL)

Diagram of IPNL effects

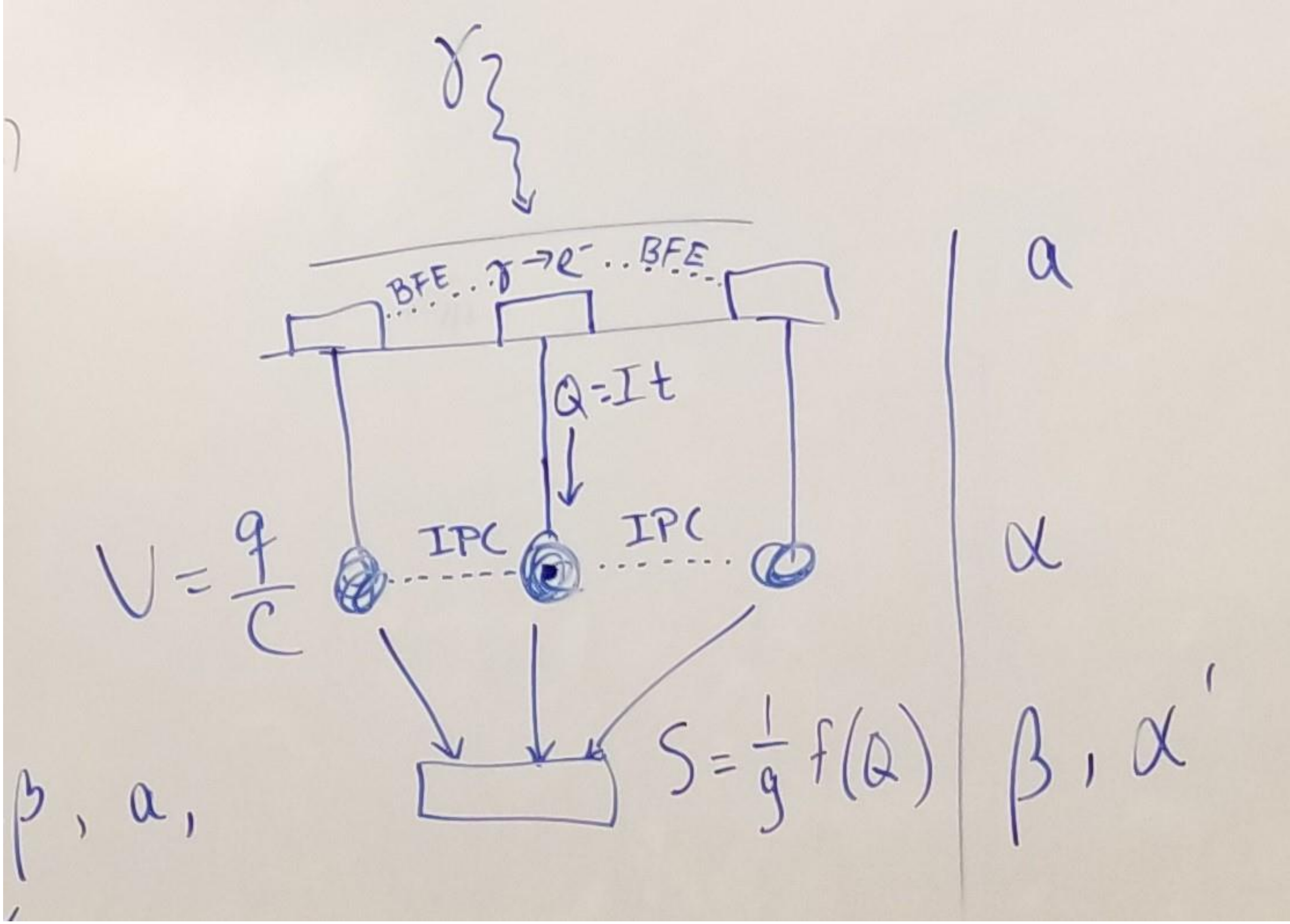

Why do we care?

- Goal of *Roman* is to optimize results of cosmic shear
- Shear signal is small, so systematic shape errors must be kept under control at $\sim 10^{-4}$ level
- IPNL impacts measurements of bright stars → get PSF → corrects shapes of galaxies
  - Errors will propagate through analysis pipeline → wrong σ_8, Ω_m

Our work

- Builds on work by Hirata & Choi to determine IPNL parameters
  - Had a lingering bias of 12% on BFE determination
- Rework their formalism in Fourier space
  - Makes it easier to include higher-order nonlinearities
- Implement changes into SOLID-WAFFLE
- Measured IPNL for 3 flight candidate detectors

The formalism (1/2)

- Signal correlation function across time slices:

$$\widetilde{C}_{abcd}(k_1' - k_1, k_2' - k_2) = \mathrm{Cov}\left[\widetilde{S}_a(k_1, k_2) - \widetilde{S}_b(k_1, k_2), \widetilde{S}_c(k_1', k_2') - \widetilde{S}_d(k_1', k_2')\right]$$

- Signal with IPC + NLIPC + CNL:

$$\widetilde{S}_a^{n,\mathrm{IPC+NLIPC+CNL}} = \frac{1}{g}\left[\widetilde{Q}_a\left(\widetilde{K} + \widetilde{K}^I\overline{Q}_a\right)\left(1 - \sum_{\nu=2}^{n}\nu\beta_\nu\overline{Q}_a^{\nu-1}\right) + N^2\delta_{k_1,0}\delta_{k_2,0}\sum_{\nu=2}^{n}\beta_\nu(\nu-1)\overline{Q}_a^{\nu}\right]$$

- BFE on charge:

$$\langle\widetilde{Q}(k_1, k_2, t+\delta t)\rangle|_t = \widetilde{Q}(k_1, k_2, t) + \Delta\widetilde{Q}(k_1, k_2, t) = \widetilde{Q}(k_1, k_2, t) + I\widetilde{W}(k_1, k_2, t)\delta t$$

The formalism (2/2)

- Covariance between different modes at different times:

$$\mathrm{Cov}\left[\widetilde{Q}(t), \widetilde{Q}'(t_1)\right] = \frac{N^2 \delta_{k+k',0}}{\widetilde{a}^* + \widetilde{a}^{*\prime} - \widetilde{a}^{*+}}\, e^{I\widetilde{a}^*(t-t_1)} \left(e^{I(\widetilde{a}^* + \widetilde{a}^{*\prime})t_1} - e^{I\widetilde{a}^{*+}t_1}\right)$$

- Full correlation function:

$$\begin{aligned}
\widetilde{C}^{\mathrm{full}}_{abcd} = \frac{1}{g^2} \Bigg[& \left(1 - \sum_{\nu=2}^{n} \nu\beta_\nu \overline{Q}_a^{\nu-1}\right)\left(1 - \sum_{\nu=2}^{n} \nu\beta_\nu \overline{Q}_c^{\nu-1}\right)\left(\widetilde{K} + \widetilde{K}^I \overline{Q}_a\right)\left(\widetilde{K}' + \widetilde{K}^{I\prime} \overline{Q}_c\right) \mathrm{Cov}\left(\widetilde{Q}_a, \widetilde{Q}'_c\right) \\
& - \left(1 - \sum_{\nu=2}^{n} \nu\beta_\nu \overline{Q}_a^{\nu-1}\right)\left(1 - \sum_{\nu=2}^{n} \nu\beta_\nu \overline{Q}_d^{\nu-1}\right)\left(\widetilde{K} + \widetilde{K}^I \overline{Q}_a\right)\left(\widetilde{K}' + \widetilde{K}^{I\prime} \overline{Q}_d\right) \mathrm{Cov}\left(\widetilde{Q}_a, \widetilde{Q}'_d\right) \\
& - \left(1 - \sum_{\nu=2}^{n} \nu\beta_\nu \overline{Q}_b^{\nu-1}\right)\left(1 - \sum_{\nu=2}^{n} \nu\beta_\nu \overline{Q}_c^{\nu-1}\right)\left(\widetilde{K} + \widetilde{K}^I \overline{Q}_b\right)\left(\widetilde{K}' + \widetilde{K}^{I\prime} \overline{Q}_c\right) \mathrm{Cov}\left(\widetilde{Q}_b, \widetilde{Q}'_c\right) \\
& + \left(1 - \sum_{\nu=2}^{n} \nu\beta_\nu \overline{Q}_b^{\nu-1}\right)\left(1 - \sum_{\nu=2}^{n} \nu\beta_\nu \overline{Q}_d^{\nu-1}\right)\left(\widetilde{K} + \widetilde{K}^I \overline{Q}_b\right)\left(\widetilde{K}' + \widetilde{K}^{I\prime} \overline{Q}_d\right) \mathrm{Cov}\left(\widetilde{Q}_b, \widetilde{Q}'_d\right) \Bigg]
\end{aligned}$$

SOLID-WAFFLE

- Takes detector flats and darks as inputs
- Returns IPNL parameters measured in super-pixels
- Compares measured correlation function to theory prediction

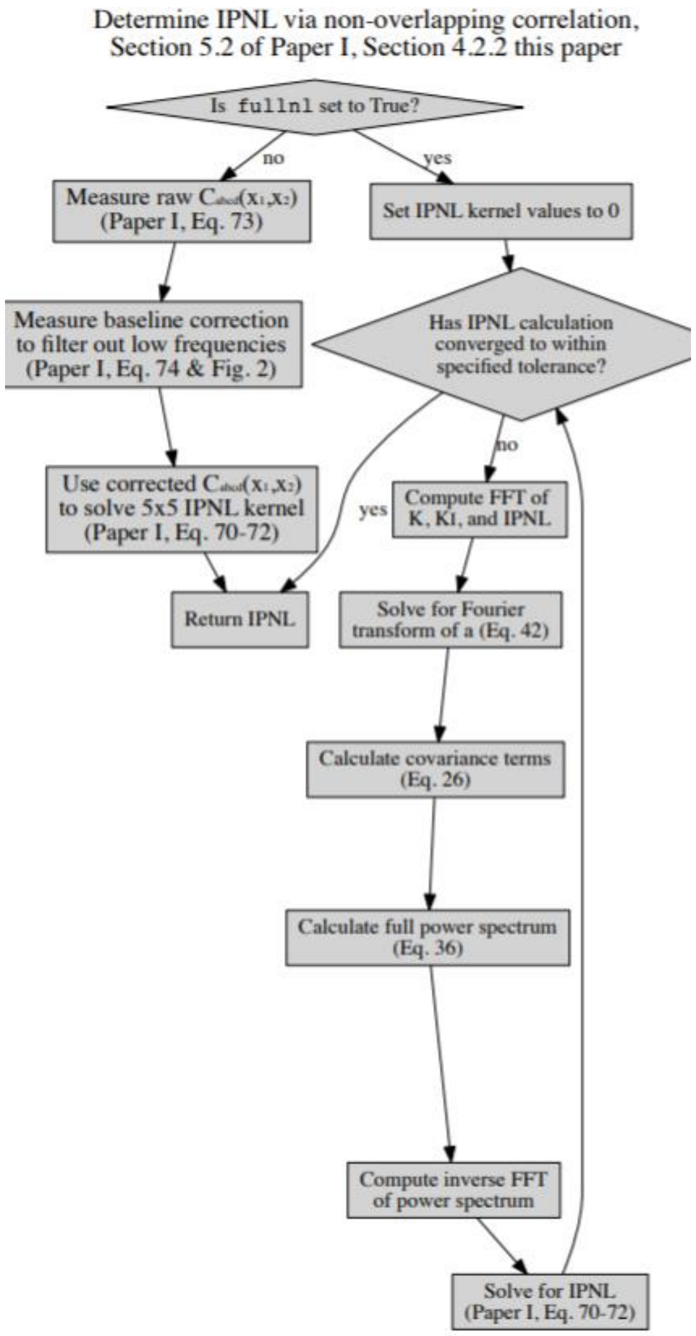

Darks and flats

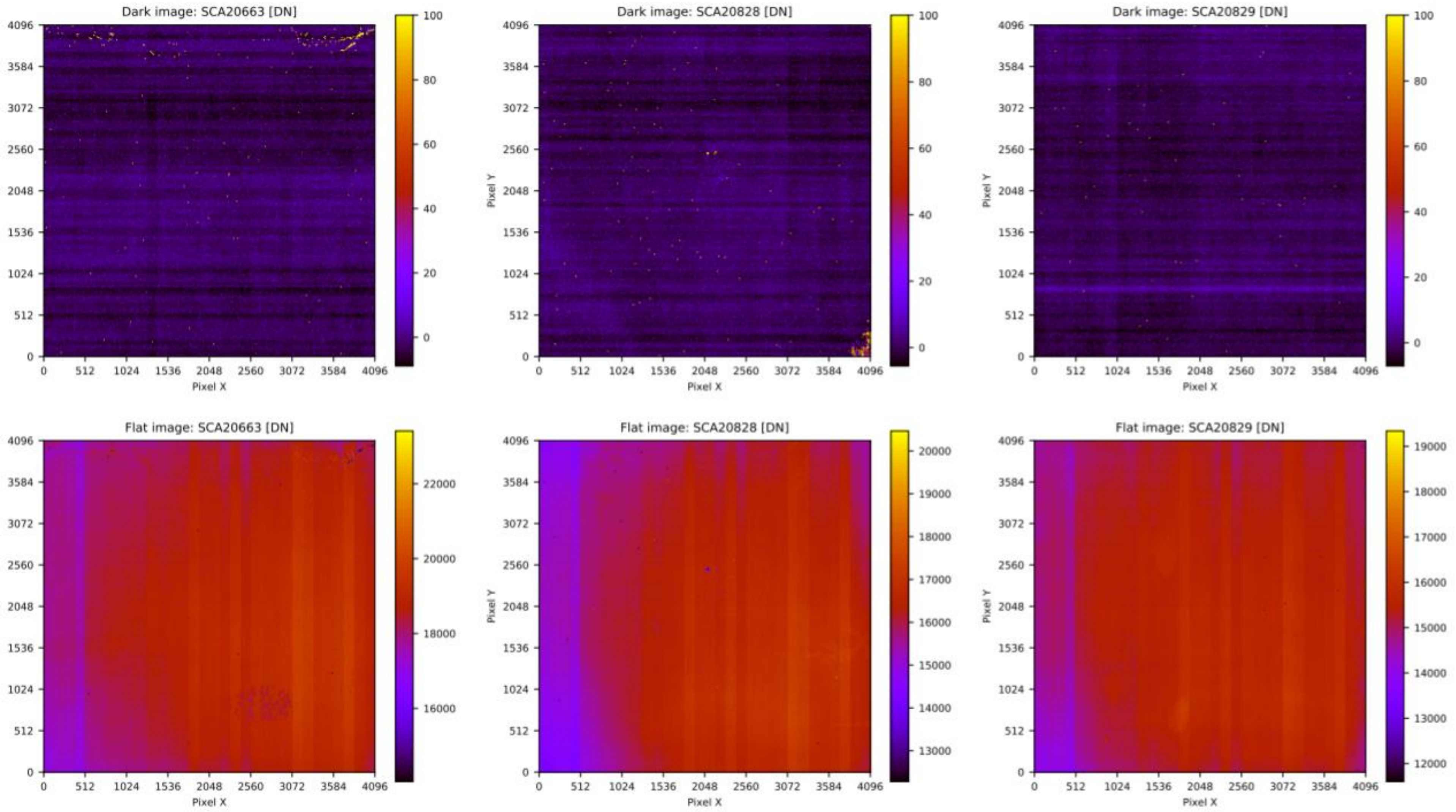

Results

- Output BFE coefficients match inputs to within 1%
- BFE dominates over NLIPC for all 3 candidates
- IPNL not symmetric in rows and columns

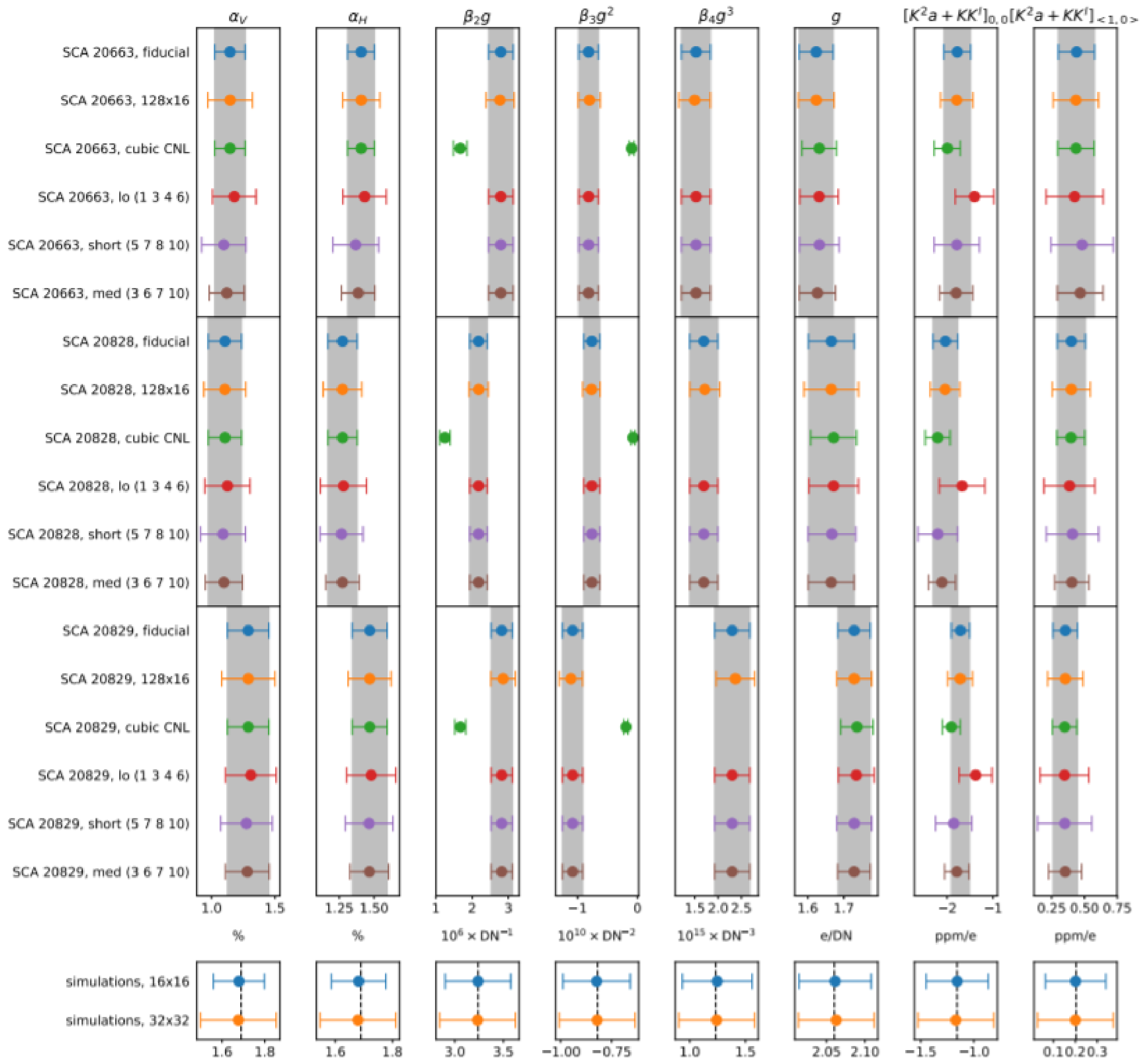

Surprise Part III (?): CMB Constraints

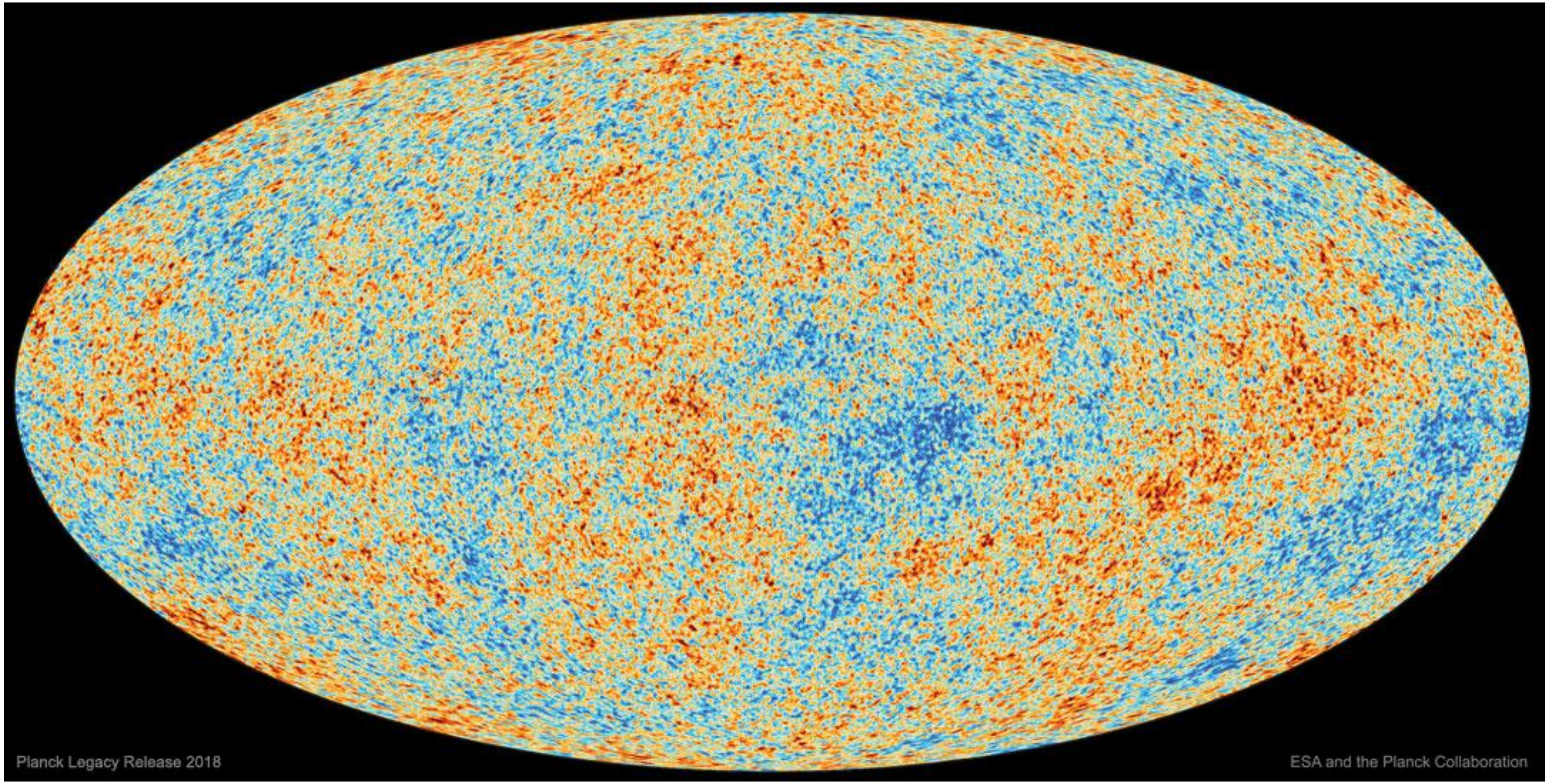

CMB application: neutrino masses (1/2)

- Expansion history changes as they become non-relativistic
  - Probes sensitive to history, like BAO, can measure the effect
- Neutrino masses suppress late-time amplitude of fluctuations
- Primary CMB spectrum and secondary CMB lensing spectrum

Suppression of power

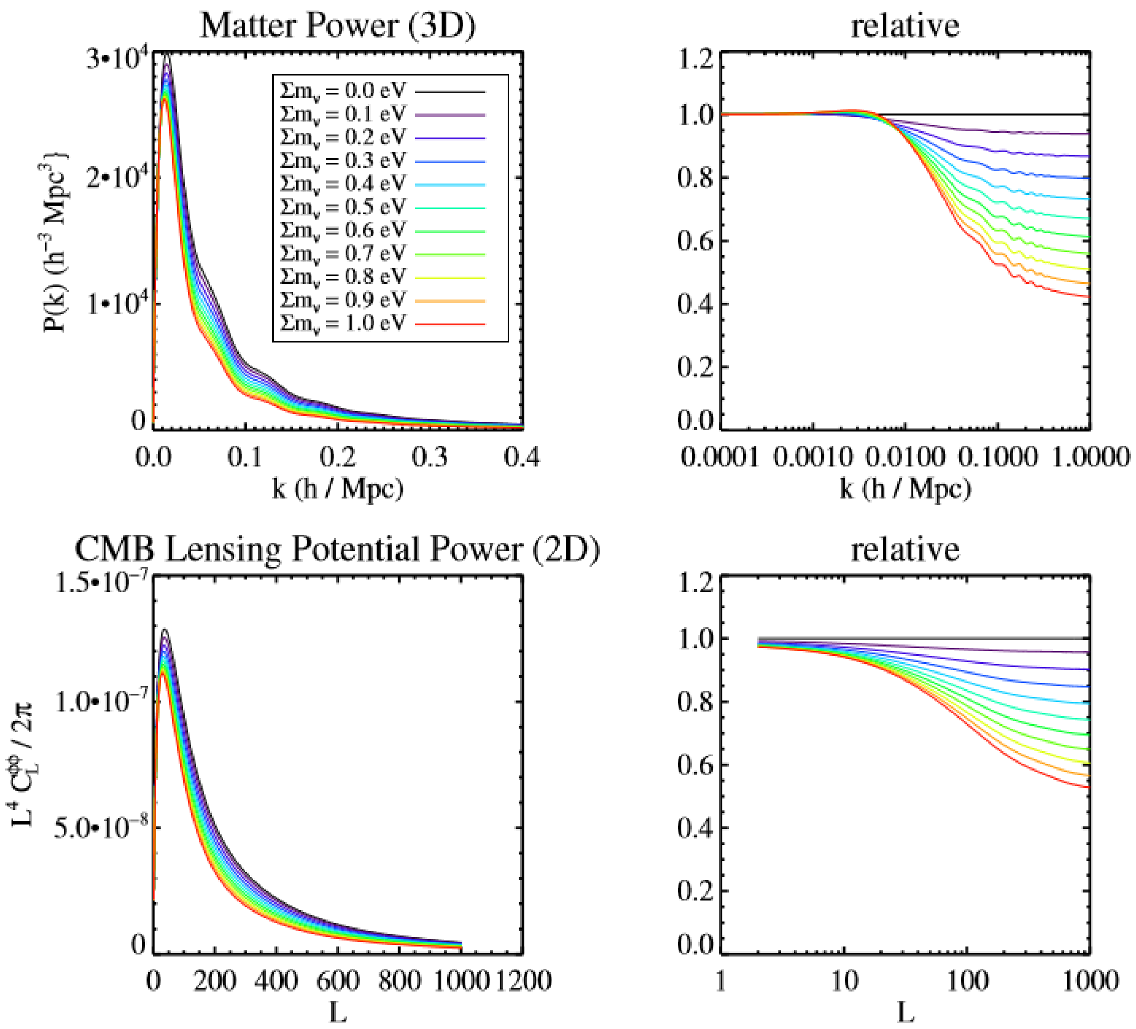

Abazajian et al. 2016 (CMB-S4 Science Book)

CMB application: neutrino masses (2/2)

- DESI BAO information helps break degeneracy of Σm_ν with Ω_m
  - Get BAO from galaxies, quasars, and Lyα forest
- SO (Goal) + DESI BAO + τ (LiteBIRD) : $\sigma(\Sigma m_\nu) = 17$ meV
  - Enable detection of $\Sigma m_\nu = 0.06$ eV at 3.5σ and $\Sigma m_\nu = 0.1$ eV at 5.9σ

Limits from Simons + DESI + τ

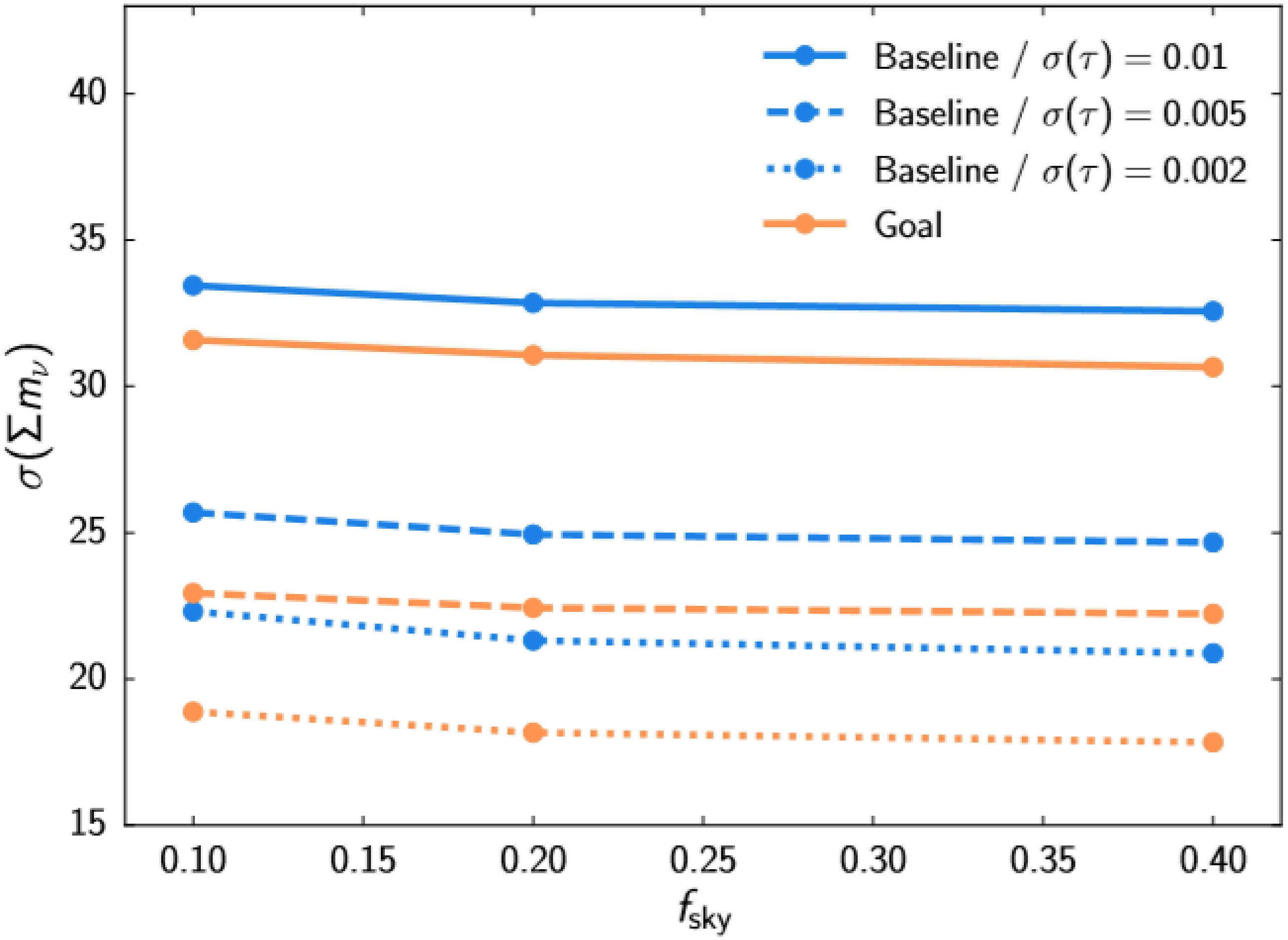

SO Collaboration, JCAP 02 (2019) 056

CMB application: primordial non-Gaussianity

- Local PNG parameterized by f_{NL}
  - Can place constraints on inflationary models
- Causes galaxies to exhibit scale-dependent bias $b(k) \propto f_{NL}/k^2$
- The same dependence is present in the Lyα forest
  - See U. Seljak, JCAP 03 (2012) 004 and S. Chongchitnan, JCAP 10 (2014) 034
- Could CMB + Lyα improve PNG constraints from CMB + galaxies?

Limits from Simons lensing + Rubin clustering

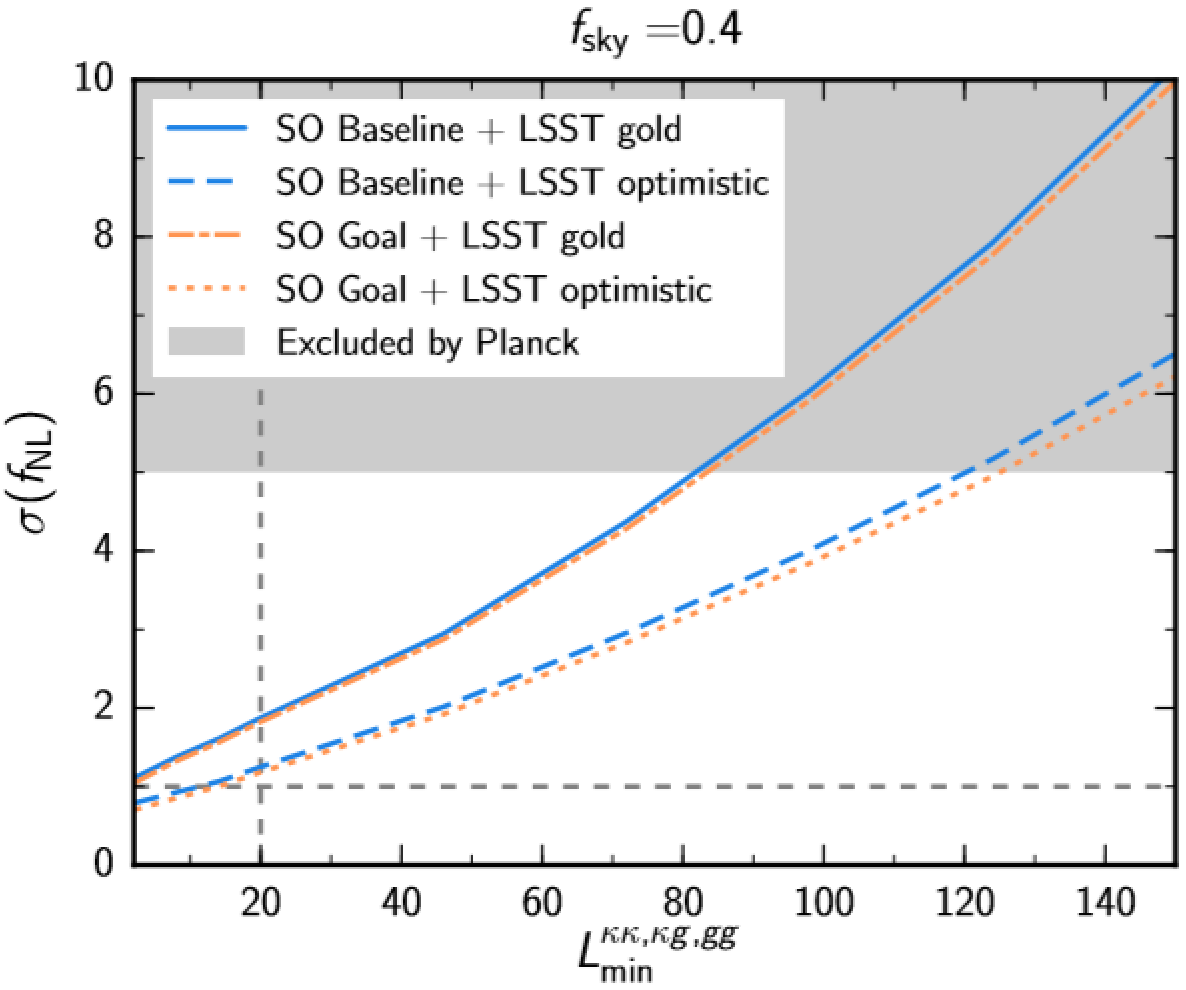

SO Collaboration, JCAP 02 (2019) 056

Conclusions

- Lyα forest is great for studying smaller scales at earlier times
- Perturbative modeling must improve to get accurate cosmology
  - In the future: complete 1-loop model and bias coefficients
- Complements CMB measurements including Σm_ν, PNG
- LSS + CMB data will help achieve unprecedented precision